Supplementary Information Guide

1. **List of Supplementary Tables 1-8**
2. **Supplementary Discussion**
3. **Supplementary Figures 1-9**

List of Supplementary Tables

Supplementary Table 1. Gene-ranking based on sgRNA enrichment analysis.

Supplementary Table 2. Gene set enrichment analysis output for top 100 ranked genes from 2CT-CRISPR screens. For the analysis, the Gene Ontology set (released 2015-08-06) was used from Panther (http://pantherdb.org/about.jsp).

Supplementary Table 3. Pathway enrichment analysis of top 554 ranked genes from 2CT-CRISPR screens.

Supplementary Table 4. List of genes from the CRISPR screen whose expression correlated with cytolytic activity in the TCGA database aligned according to each cancer type.

Supplementary Table 5. Genes intersected from the CRISPR screen and the TCGA database that associated with cytolytic activity clustered according to their association commonality across 36 different cancer datasets.

Supplementary Table 6. Pearson correlation of 19 genes strongly associated with CYT across majority of TCGA tumour types.

Supplementary Table 7. List of genes and sgRNA spacers used in validation screens.

Supplementary Table 8. List of PCR primers used for indel analyses.

Supplementary Discussion

The 2CT-CRISPR model preserves several important aspects of T cell biology and cancer immunotherapy. First, T cells recognize and clear tumours that express neoantigens arising from somatic mutations in the context of both adoptive cell transfer and immune checkpoint

blockade therapy, indicating that direct antigen recognition on tumours is involved in this process.[1-3] Second, CRISPR-based knock-out of *B2m* in B16 tumours abrogated the tumour clearance mediated by ACT of Pmel-1 T cells (Fig. 5i, j). Third, emerging clinical data shows that tumour cells that contain defects in antigen presentation components like β2M and HLA are associated with resistance to immune checkpoint blockade and adoptive transfer of mutation-reactive tumour infiltrating T cells (TIL) therapies[4-6]. Although our study focuses primarily on the genes that must be expressed by tumour cells to enable recognition and killing by T cells, it sheds light on several factors and processes that may be relevant to the fundamental interactions between T cells and their target cells in normal immunobiology.

Insights into validated CRISPR screen hits

Validated hits from our screens with recurrent mutations in patient tumours suggests a causal role in immune escape. For instance, CD58 was not only ranked in the top 20 enriched genes in our screens (Fig. 2d) but was also validated across melanomas, antigens and cancers (Fig. 4). CD58 is mutated or aberrantly expressed in >60% of diffuse large B cell lymphomas (Extended Fig. 5d)[7]. CD58 binds to CD2 molecule on T cells to stabilize the immune synapse formation between T cells and antigen presenting cells (APCs), acting as a co-stimulator[8]. Here, our data suggests that loss-of-function mutations in CD58 may result in immune evasion from T cell mediated cytotoxicity, even in epithelial malignancies.

SOX10 is a transcription factor reported to be necessary for melanomagenesis[9]. It has ~16-fold higher expression in melanoma over virtually every other kind of cancer (Supplementary Fig. 2). To understand the effect of SOX10 in regulation of EFT in our melanoma cell lines, we used the TRRUST TF target database[10] (http://www.grnpedia.org/trrust/) to find SOX10 targets. For SOX10, TRRUST identifies 11 unique target genes of SOX10, including the well-known melanoma gene MITF. The other targets are: COL11A2, EDNRB, GJB1, GJC2, MBP, MIA,

MPZ, NES, PMP22, and RET. Of these 11 SOX10 target genes, 8 genes have a CRISPR screen rank (via RIGER analysis) in the top 25% of our screen hits, implying that loss of expression of any of these genes has a resistance effect and that with SOX10 loss there is potentially decreased expression of many of these genes. For example, MITF has a RIGER rank of 342, which is in the top 2% of all genes in the library (342/21915 = ~1.5%). Thus, many of the SOX10 target genes are enriched in our CRISPR screen indicating that this transcription factor has an additional role in regulation of EFT. Recently, others have shown that loss of SOX10 through mutation or epigenetic silencing is a key early step in acquired drug resistance in melanoma[11].

BBS1 was enriched in our 2CT-CRISPR screens with low selection pressure (E:T of 0.3) (Extended data Fig. 4d). It was validated in multiple cell lines and cancers to be important for the regulation of EFT (Fig. 4, Extended data Fig. 6). BBS1 loss in tumours did not change the amount of IFNγ release in 2CT assay indicating BBS1 loss resisted EFT without affecting the recognition of tumours by T cells (Supplementary Fig. 5). BBS1 is canonically a part of BBSome complex that regulates ciliary trafficking and sonic hedgehog (SHH) pathway[12]. BBS1 loss has been shown to disrupt proteosomal functions and Wnt signalling in eukaryotic cells[13]. Recently it has been reported that Wnt signalling disruption in tumours can cause immune evasion from NK cell mediated cytolysis through downregulation of ULBP ligands (innate immune sensors)[14]. This association of BSS1 and Wnt signalling with immune evasion warrants further investigation to understand if this interaction is relevant in modulation of T cell mediated cytolysis.

Core genes such as *RPL23* and *RPL10A* essential for cell survival and proliferation[15] were significantly enriched in these CRISPR screens. To address whether any of these genes are indeed lethal to Mel624 cells, we included *RPL23* in our arrayed validation studies. *RPL23* perturbation with all four sgRNAs was tolerated in Mel624 cells while two of sgRNAs were lethal

in A375 cells within 7 days of introduction in cell cultures (Fig. 4b, Extended Fig. 6a). We also analysed the extent of sgRNA depletion of these genes in long term cultured cells (day 17) post CRISPR library transduction, and found *RPL10A* and *RPL23* to be ranked 49 and 26 by RIGER analysis in Mel624 cells (Supplementary Table 1). However, RLP23-pertubed cells resisted T cell mediated lysis (Figs. 4b-c) when subjected to 2CT assay within 10 days of lentiCRISPR infection indicating that RPL23 is a bona fide regulator of EFT.

In addition, we observed an interesting bias in enrichment of 60S versus 40S ribosomal genes. Out of 102 ribosomal genes targeted using the CRISPR library, 47 encoded for components of the 40S subunit and 55 encoded for 60S subunit. We found that 60S ribosomal genes (38%) are significantly enriched more than 40S ribosomal genes (6.3%) in top 500 ranked genes ($P < 0.0001$, two tailed *F-test*), suggesting that 60S ribosome in tumour cells may have an additional role in regulation of EFT. Other groups have also described a potential role of the 60S ribosome and associated proteins in oncogenesis[16,17]. Together, these data indicate that redundant mechanisms might be existing in certain tumours to circumvent such genetic lethality with 60S ribosomal genes, and that there is some shared biological role in immune evasion through impaired 60S ribosomal gene products.

The proteosomal subunit PSMB5 was also among the 14 validated genes in melanoma cells targeted with ESO T cells (Fig. 4b-c). PSMB5, encodes for the 20S proteasome subunit beta-5, is present in the canonical proteasome but not in the immunoproteasome. This suggests that the canonical 20S proteasome instead of the immunoproteasome may be involved in fragmentation of NY-ESO-1 antigen into peptides for MHC Class I presentation. This finding is supported by our observation that loss of the immunoproteosomal component LMP2 in Mel624 cells provided minimal protection against T cell mediated lysis (Extended Fig. 3c). In agreement, LMP2 has been reported to be functionally redundant for efficient antigen presentation with

other proteosomal subunits[18]. Together, these results demonstrate the unique capability of 2CT-CRISPR screens to capture differences in antigen presentation by tumour cells and APCs.

Association of top CRISPR hits with response rates to immunotherapy

In the 2CT-CRISPR screen, Cas9-induced loss-of-function (LoF) mutations in genes involved in regulation of EFT lead to resistance to T cell-mediated lysis (Fig. 2d-e, 4b-d). To test whether there is an association between the genes from the pooled screen and patient responses to immunotherapy, we measured the enrichment of LoF mutations in these genes in pre-treatment tumours from immune checkpoint blockade antibody-treated melanoma patients from three recently published genomic datasets (Van Allen *et al.*[2], Roh *et al.*[19] and Hugo *et al.*[20] cohorts).

For our analysis, we counted nonsense, frameshift, in-frame insertions/deletions, non-stop, start out-of-frame and splice-site mutations from the patient tumour exome sequencing data as LoF mutations (exome data from Van Allen *et al.* Table S1, Hugo *et al.* Table S1D, and Roh *et al.* Table S4). This yielded 7,591 LoF mutations total from all 3 datasets combined. We also included phenotypic data that classified each patient as a responder or non-responder after anti-CTLA4 or anti-PD1 immunotherapy. When ordering genes by their RIGER rank from the 2CT-CRISPR screen, we found that the cumulative sum of LoF mutations in non-responders divided by the cumulative sum of LoF mutations in responders is >1 for top-ranked genes from the 2CT-CRISPR screen, indicating an enrichment of mutations in these genes in non-responders (Supplementary Fig. 8). In contrast, we did not find a similar enrichment when considering all mutations (e.g. missense and synonymous) from these patient datasets.

Given that the enrichment persists over roughly the first 200 RIGER-rank genes, we computed the overlap between these genes and all genes with a bias towards non-responders. Specifically, we found 605 genes which had more LoF mutations in non-responders over

responders (defined as at least 2 more LoF mutations in non-responders than in responders). Between these 605 genes and the top 200 RIGER-rank genes, we found an overlap of 10 genes (P = 0.03, hypergeometric test), including several with established roles in immune response and oncogenesis (*APLNR, B2M, BRAF, CENPF, NIPBL, OTC, PLD3, RAD1, RIPK1, SEMA6B*). Despite the small size of the genomic datasets (n = 204 patients when pooling responders and non-responders from all three studies together) and the limitations of pre-treatment exome sequencing from genetically heterogenous tumour biopsies, it is encouraging to see agreement between the 2CT-CRISPR assay and LoF mutations in tumours from non-responders.

Supplementary References

1 Tran, E. *et al.* Immunogenicity of somatic mutations in human gastrointestinal cancers. *Science* **350**, 1387-1390 (2015).

2 Van Allen, E. M. *et al.* Genomic correlates of response to CTLA-4 blockade in metastatic melanoma. *Science* **350**, 207-211 (2015).

3 Schumacher, T. N. & Schreiber, R. D. Neoantigens in cancer immunotherapy. *Science* **348**, 69-74 (2015).

4 Zaretsky, J. M. *et al.* Mutations associated with acquired resistance to PD-1 blockade in melanoma. *New England Journal of Medicine* **375**, 819-829 (2016).

5 Tran, E. *et al.* T-cell transfer therapy targeting mutant KRAS in cancer. *New England Journal of Medicine* **375**, 2255-2262 (2016).

6 Le, D. T. *et al.* Mismatch-repair deficiency predicts response of solid tumors to PD-1 blockade. *Science*, aan6733 (2017).

7 Challa-Malladi, M. *et al.* Combined genetic inactivation of β2-microglobulin and CD58 reveals frequent escape from immune recognition in diffuse large B cell lymphoma. *Cancer Cell* **20**, 728-740 (2011).

8 Dustin, M. L. & Cooper, J. A. The immunological synapse and the actin cytoskeleton: molecular hardware for T cell signaling. *Nat Immunol* **1**, 23-29 (2000).

9 Shakhova, O. *et al.* Sox10 promotes the formation and maintenance of giant congenital naevi and melanoma. *Nat Cell Biol* **14**, 882-890 (2012).

10 Han, H. *et al.* TRRUST: a reference database of human transcriptional regulatory interactions. *Scientific Reports* **5**, 11432 (2015).

11 Shaffer, S. M. *et al.* Rare cell variability and drug-induced reprogramming as a mode of cancer drug resistance. *Nature* **546**, 431-435 (2017).

12 Su, X. *et al.* Bardet–Biedl syndrome proteins 1 and 3 regulate the ciliary trafficking of polycystic kidney disease 1 protein. *Human Molecular Genetics* **23**, 5441-5451 (2014).

13 Gerdes, J. M. *et al.* Disruption of the basal body compromises proteasomal function and perturbs intracellular Wnt response. *Nat Genet* **39**, 1350-1360 (2007).

14 Malladi, S. *et al.* Metastatic latency and immune evasion through autocrine inhibition of WNT. *Cell* **165**, 45-60 (2016).

15 Hart, T. *et al.* High-resolution CRISPR screens reveal fitness genes and genotype-specific cancer liabilities. *Cell* **163**, 1515-1526 (2015).

16 Sulima, S. O. *et al.* Bypass of the pre-60S ribosomal quality control as a pathway to oncogenesis. *Proceedings of the National Academy of Sciences* **111**, 5640-5645 (2014).

17 Fancello, L., Kampen, K. R., Hofman, I. J., Verbeeck, J. & De Keersmaecker, K. The ribosomal protein gene RPL5 is a haploinsufficient tumor suppressor in multiple cancer types. *Oncotarget* **8**, 14462-14478 (2017).

18 Yewdell, J., Lapham, C., Bacik, I., Spies, T. & Bennink, J. MHC-encoded proteasome subunits LMP2 and LMP7 are not required for efficient antigen presentation. *The Journal of Immunology* **152**, 1163-1170 (1994).

19 Roh, W. *et al.* Integrated molecular analysis of tumor biopsies on sequential CTLA-4 and PD-1 blockade reveals markers of response and resistance. *Science Translational Medicine* **9**, aah3560 (2017).

20 Hugo, W. *et al.* Genomic and transcriptomic features of response to anti-PD-1 therapy in metastatic melanoma. *Cell* **165**, 35-44 (2016).

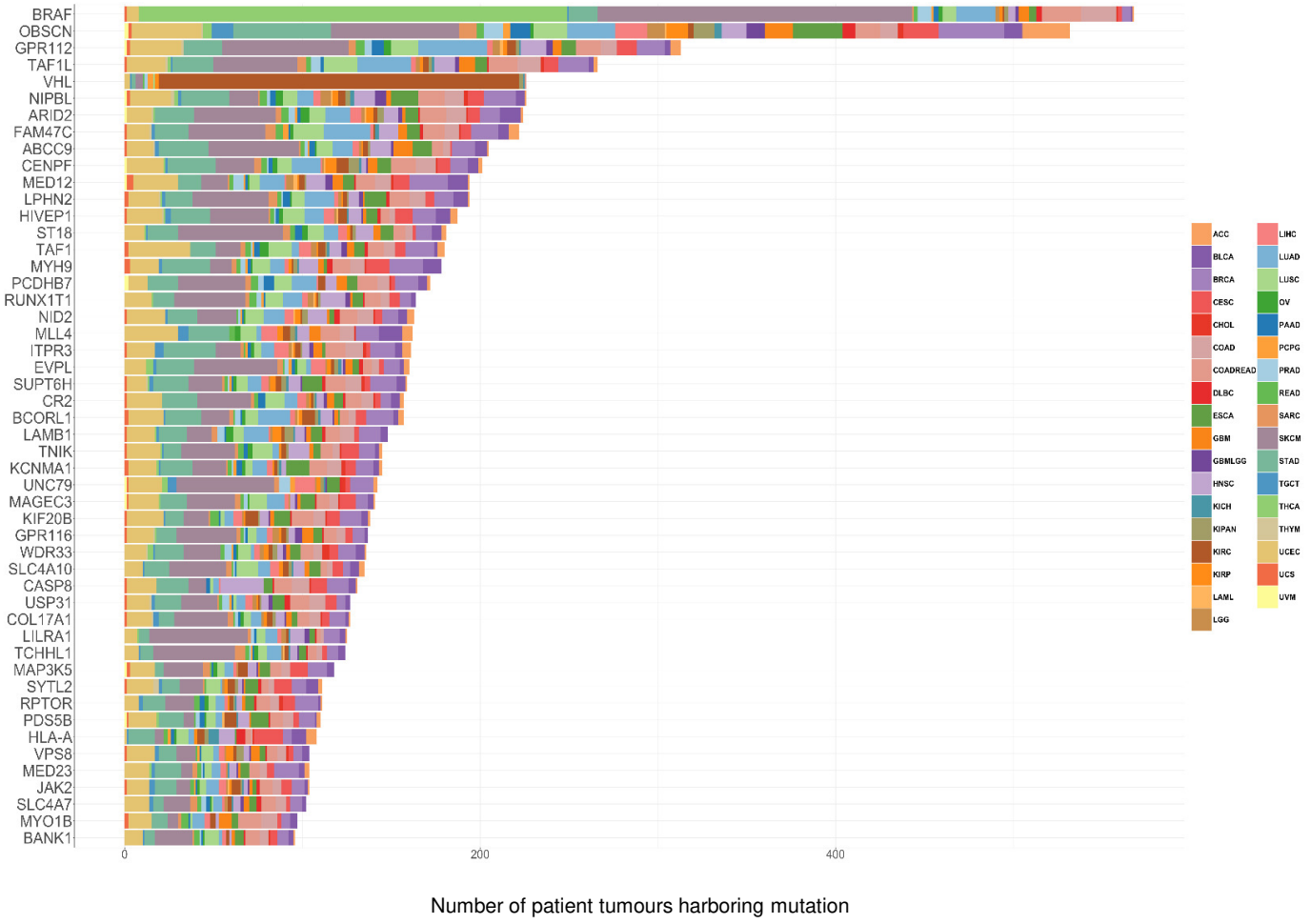

Supplementary Figure 1. Pan-cancer mutational heterogeneity of top 200 candidate genes from the 2CT-CRISPR screen with T cell selection at E:T of 0.5. For each gene, patient tumour data from each TCGA sample set showing genetic aberrations (including missense, nonsense, frameshift, truncation, splice-site mutations, and homozygous deletions).

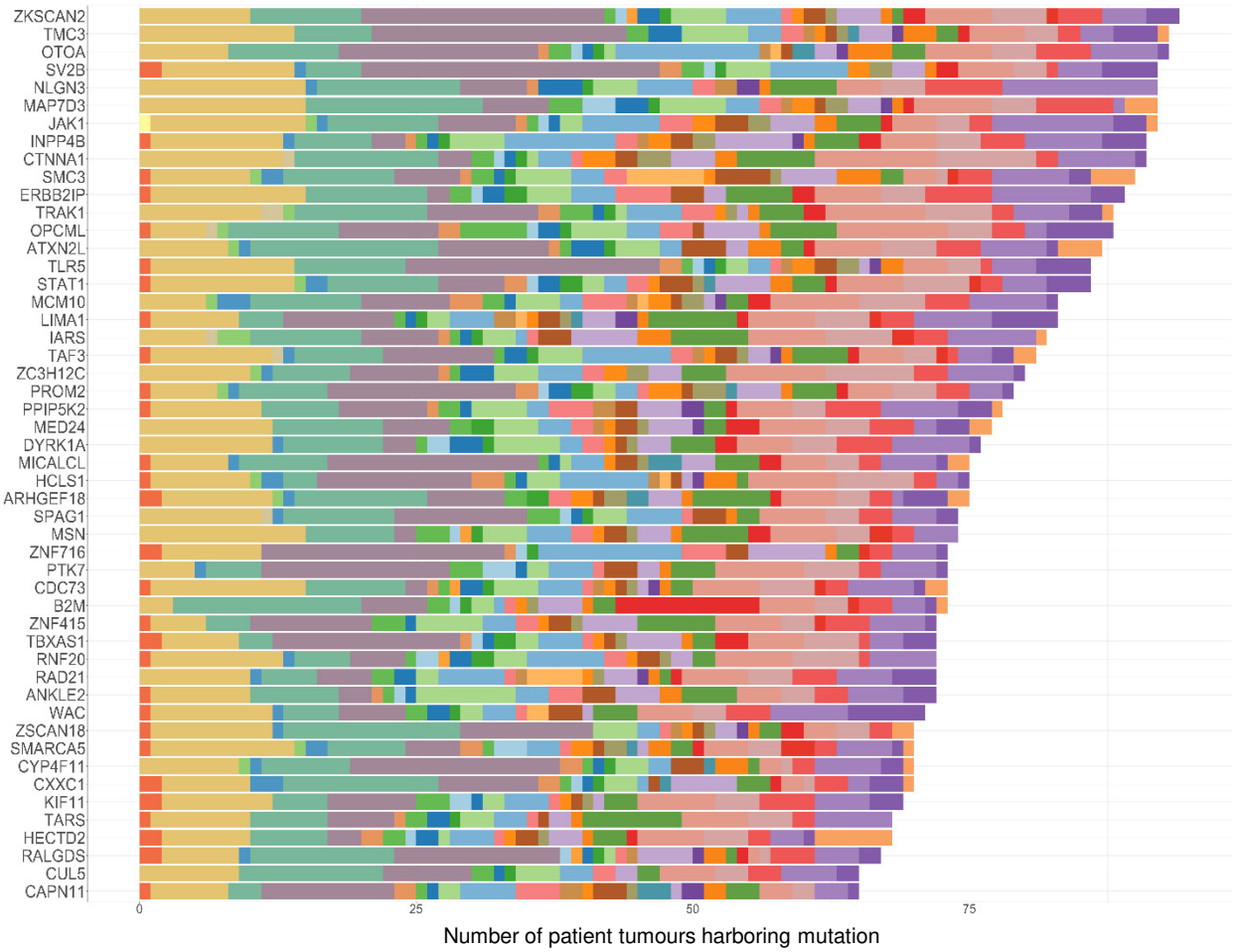

Supplementary Figure 1. Continued

Supplementary Figure 1. Continued

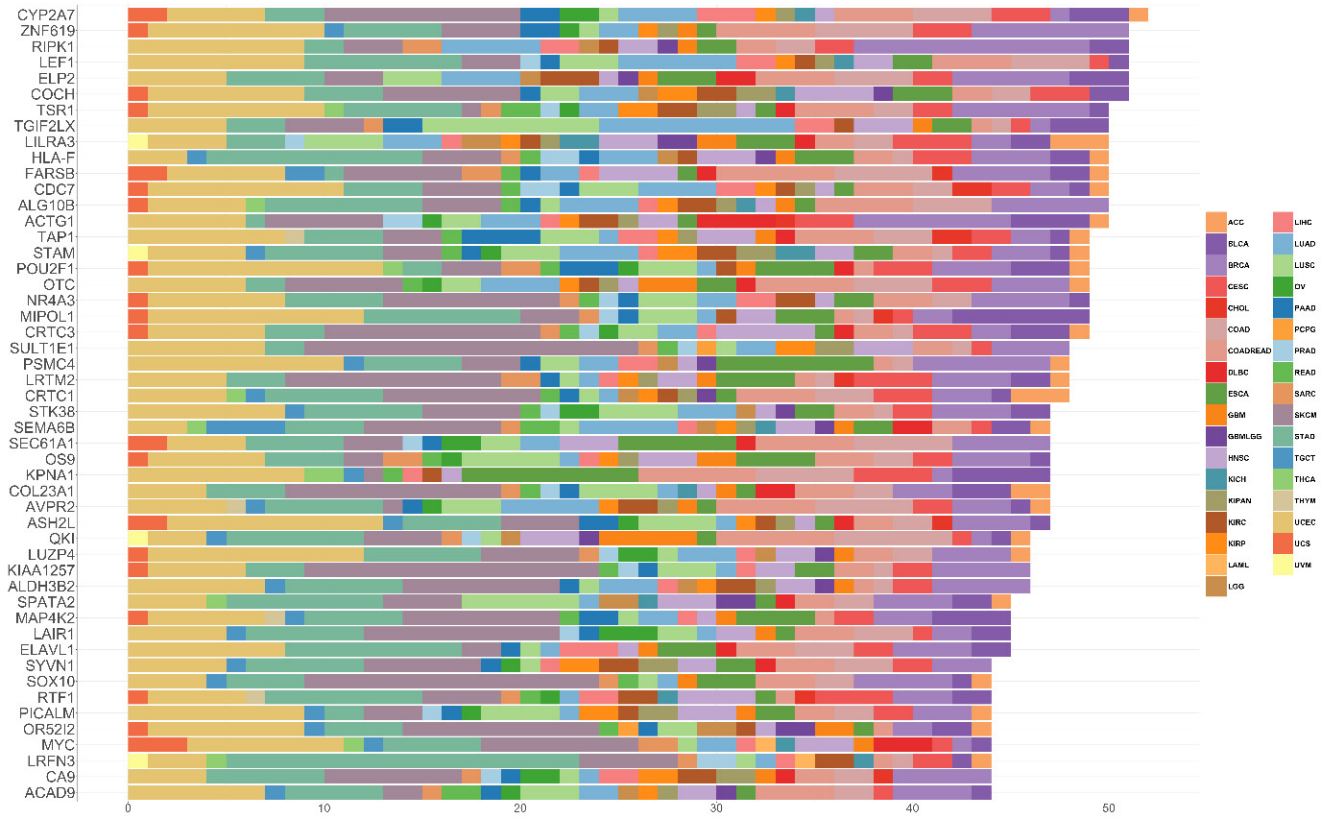

Supplementary Figure 1. Continued

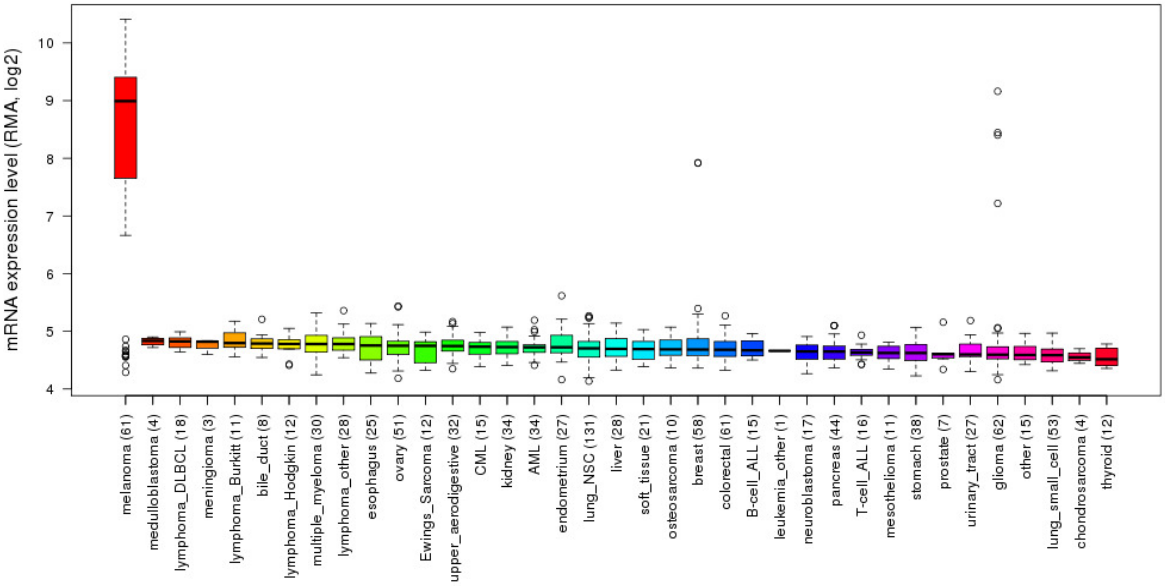

Supplementary Figure 2. Expression of the transcription factor SOX10 across multiple cancer-types from the Broad-Novartis Cancer Cell Line Encyclopedia. (*n* = 1,036 cell lines across all cancer types[57]).

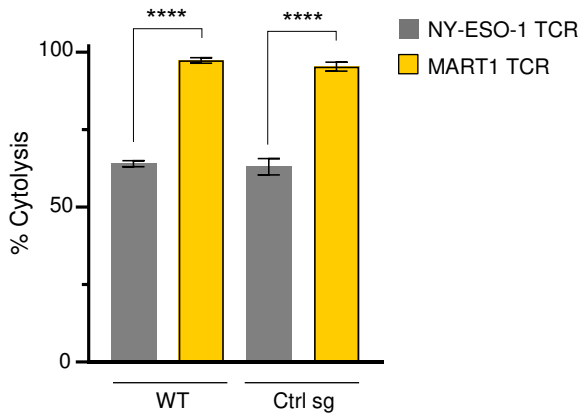

Supplementary Figure 3. Differential cytolytic ability of T cells transduced with NY-ESO-1 TCR versus MART1 TCR against Mel624 cells. Data is represented as an average of three technical replicates. **** $P < 0.0001$. T cells were co-cultured with tumor cells at E:T of 1.0 for 24 h.

a

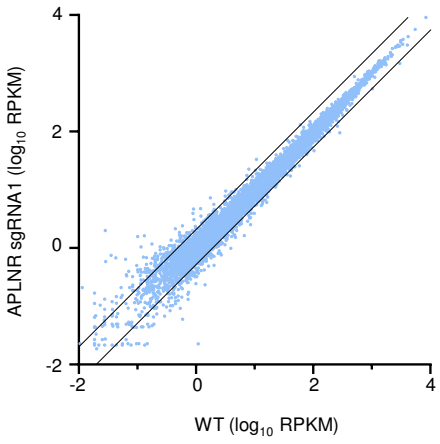

b

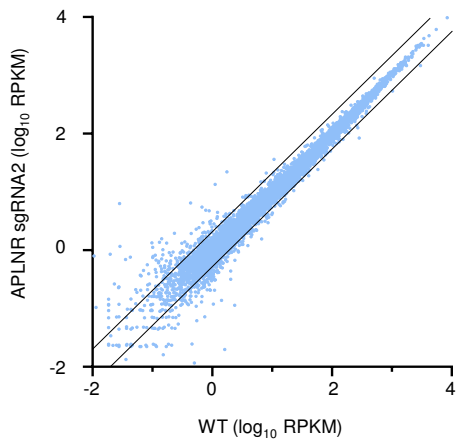

c

Upregulated Genes

	APLNR-sgRNA1 vs WT		APLNR-sgRNA2 vs WT	
Gene	*P*- value	Fold change	*P*- value	Fold change
KRTAP2-3	5.81E-09	4.07	5.8E-05	2.28
ANKRD1	1.76E-19	3.37	1.3E-18	3.08
C15orf54	5.35E-06	2.85	4.7E-06	2.64
CALB1	1.67E-04	2.80	4.0E-04	2.39
KLK6	2.73E-05	2.57	6.4E-05	2.41
NOG	1.06E-06	2.54	3.1E-04	1.83
ADRB2	7.59E-05	2.46	3.9E-03	1.90
HAPLN1	2.24E-08	2.38	8.6E-08	2.24
KRT14	1.76E-06	2.26	1.6E-05	2.02
MARCH7	6.56E-05	2.23	1.7E-04	1.98
TM4SF18	4.69E-06	2.17	6.1E-06	2.17
RP11-554I8.2	2.73E-06	2.16	1.8E-05	2.00
KRT6B	3.74E-07	2.16	1.2E-06	2.04
SLC35F1	1.64E-06	2.08	7.6E-08	2.39
CYR61	4.06E-13	2.04	3.6E-13	2.04
CTGF	1.09E-12	2.02	2.2E-10	1.74

d

Downregulated Genes

	APLNR-sgRNA1 vs WT		APLNR-sgRNA2 vs WT	
Gene	*P*- value	Fold change	*P*- value	Fold change
NXPE2	8.4E-05	-3.57	3.25E-04	-2.97
STC1	8.3E-13	-3.39	1.39E-11	-3.00
PADI3	3.1E-05	-2.50	6.07E-04	-2.04
ITGA8	1.7E-04	-2.40	4.72E-04	-2.24
PCSK1	2.8E-10	-2.40	1.34E-09	-2.26
AFF2	2.6E-05	-2.37	8.94E-05	-2.20
PCDH7	4.7E-08	-2.36	3.43E-09	-2.66
GRIP1	5.6E-06	-2.35	1.37E-05	-2.28
VAV3	1.7E-04	-2.32	6.74E-05	-2.52
PTPRO	3.3E-07	-2.26	3.38E-07	-2.30
CDH7	7.4E-05	-2.20	4.17E-04	-1.98
AKAP6	9.1E-04	-2.18	6.89E-03	-1.83
MMP1	9.4E-15	-2.16	4.66E-12	-1.82
AREG	1.7E-03	-2.13	5.41E-03	-1.89
BOC	1.4E-04	-2.11	7.89E-05	-2.19
GEM	3.2E-11	-2.07	4.52E-08	-1.68

Supplementary Figure 4. Genome-scale transcriptomic analysis of *APLNR-edited* A375 cells using RNA-seq. a, Scatterplot showing the global transcriptomic profile of unedited (WT) cells compared to APLNR-sgRNA1-edited A375 cells. **b**, Scatterplot showing the global transcriptomic profile of WT cells compared to APLNR-sgRNA2. **c,** Genes significantly upregulated in APLNR-perturbed cells compared to WT cells. **d,** Genes significantly downregulated in APLNR-perturbed cells compared to WT cells. Data is represented as an average of three technical replicates.

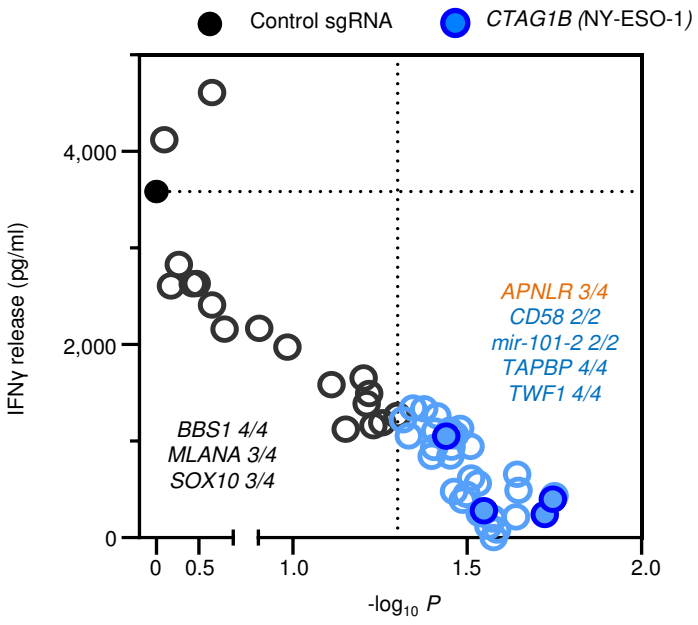

Supplementary Figure 5. Volcano plot displaying IFNγ release from T cells in the supernatants of the co-culture with gene-perturbed A375 cells after 24 h. Data representative as an average of *n* = 3 co-culture replicates. Numbers on the side of gene symbols represents 'the number of sgRNAs causing significant reduction in IFNγ release'/ 'total of sgRNAs tested'. Significance threshold is $P < 0.05$ (-log $P > 1.3$) determined by two-tailed Student t-test.

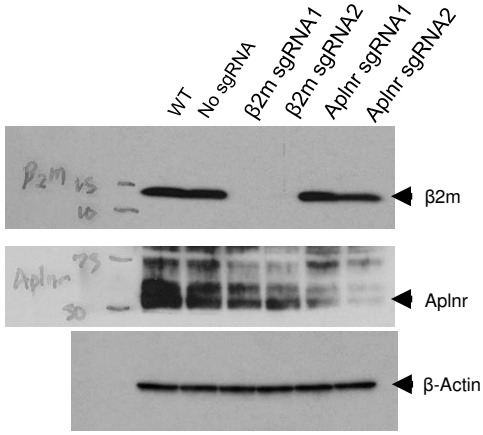

Supplementary Figure 6. Validation of CRISPR mediated gene perturbation in B16 murine melanoma cells. Western blot analysis performed on murine B16 melanoma cells to test the gene perturbation efficiency of Cas9 sgRNAs (whole blots).

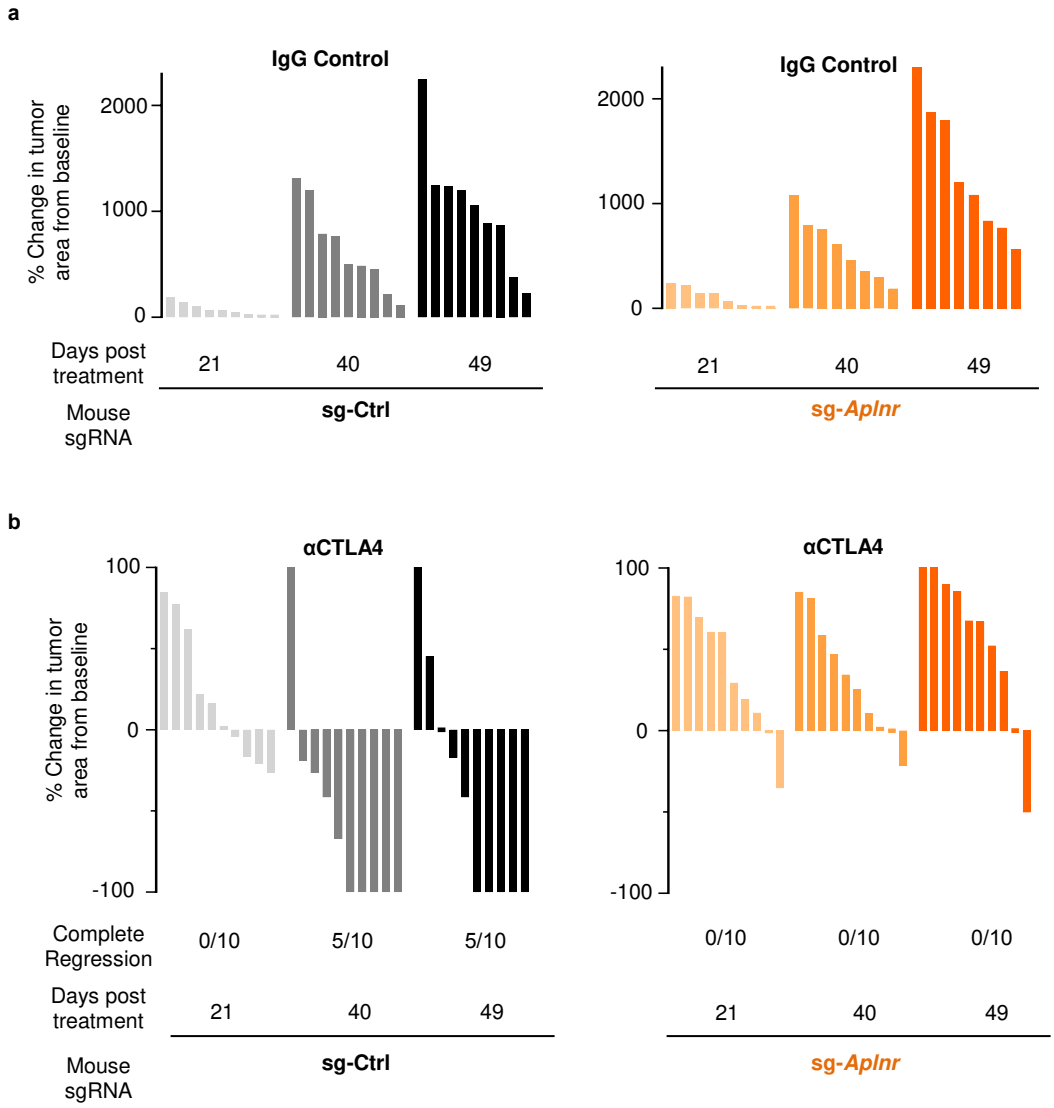

c

	Complete Regression			Progressive tumor		
	sg-Ctrl	sg-*Aplnr*	*P* value (F-test)	sg-Ctrl	sg-*Aplnr*	*P* value (F-test)
Day 40	5/10	0/10	0.0325	1/10	7/10	0.0198
Day 49	5/10	0/10	0.0325	2/10	8/10	0.023

Supplementary Figure 7. CRISPR targeting of *Aplnr* in B2905 melanoma reduces the efficacy of anti-CTLA4 treatment *in vivo*. Waterfall plots of percent change in tumor area from baseline (tumor measurements from the first day of antibody injections) to tumors measured on days 21, 40 and 49 post treatment of IgG control (panel **a**) or anti-CTLA4 (panel **b**) antibodies. B2905 melanoma cells (derived from C57BL/6-HGF mice) were subcutaneously implanted and treated with four doses of 250 µg of IgG control or anti-CTLA4 antibodies on days 10, 13, 16 and 19 post-implantation. **c,** Significance of treatment efficacy was determined by Fisher's exact test comparison of sg-Ctrl versus sg-*Aplnr* groups treated with anti-CTLA4 using the number of progressing tumors and completely regressed tumors in each group. *n* = 8/9 mice for IgG groups. *n* = 10 mice for anti-CTLA4 groups.

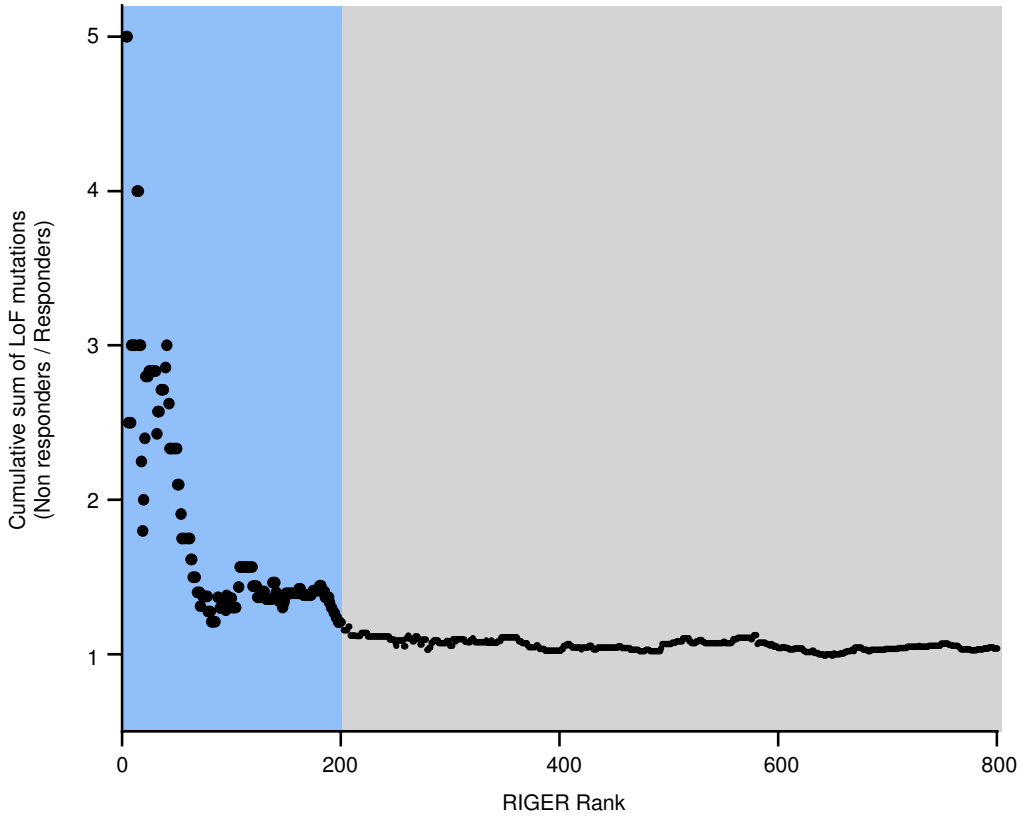

Supplementary Figure 8. Enrichment of loss-of-function mutations in top ranked CRISPR genes in non-responder versus responder patients to cancer immunotherapy.

Fig. 5d

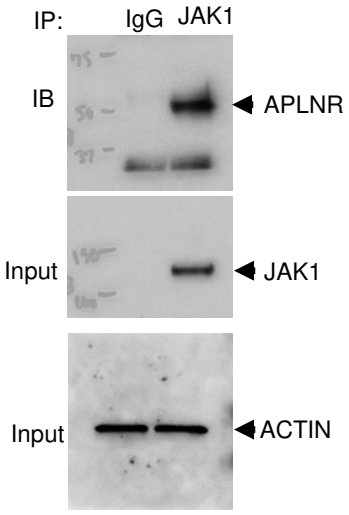

Ext. Fig. 9a

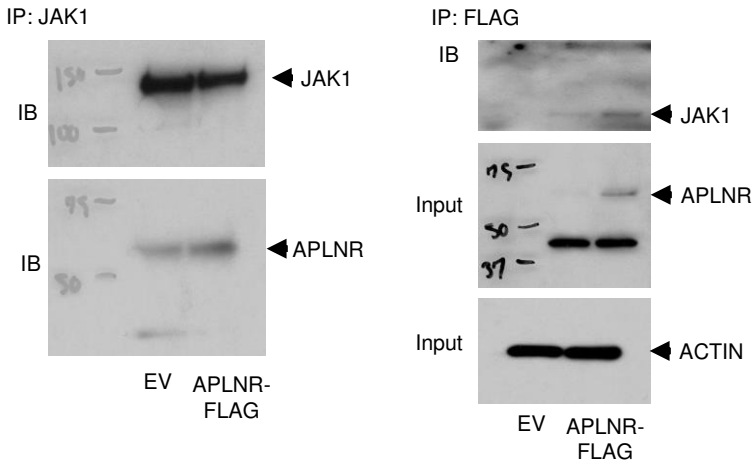

Ext. Fig. 9b

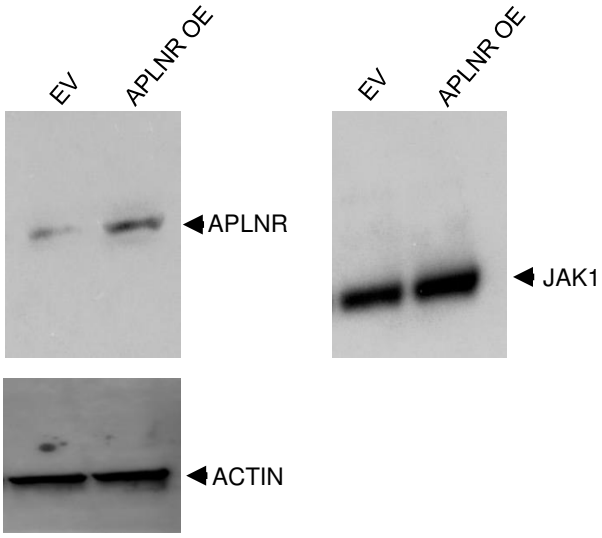

Ext. Fig. 9d

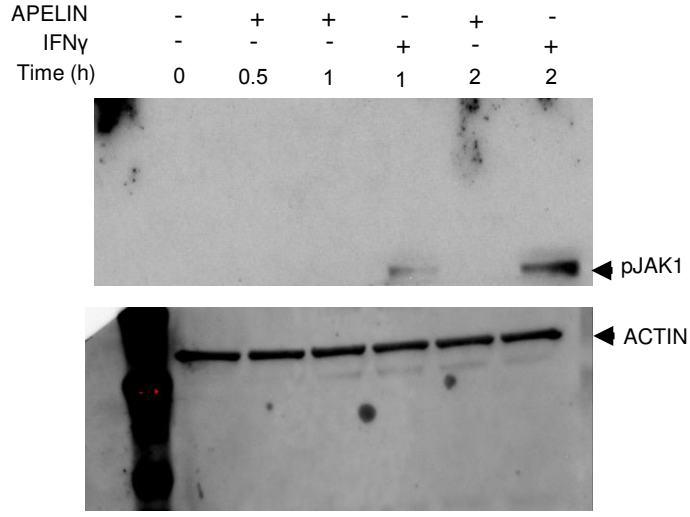

Ext. Fig. 9e

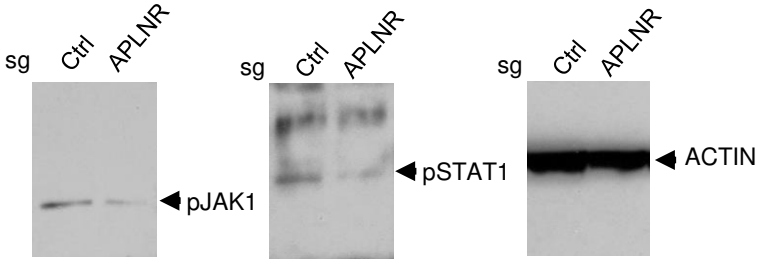

Supplementary Figure 9. Whole blots from Western and immunoprecipitation analyses of cells. Figures using these blots are indicated above each blot.